RSC Advances

ROYAL SOCIETY OF CHEMISTRY

www.rsc.org/advances

Journal Name

RSCPublishing

PAPER

Porous hollow CuS nanospheres with prominent peroxidase-like activity as large scale prepared by a one-pot controllable hydrothermal step

Qun Wei Shu,[a,c] Chun Mei Li,[b] Peng Fei Gao,[b] Ming Xuan Gao,[a] Cheng Zhi Huang*[a,b]

Cite this:

Received ooth January 2012,
Accepted ooth January 2012

DOI: 10.1039/xoxxooooox

www.rsc.org/

CuS materials with peroxidase activity have been prepared but greatly limited by the large dosage and low peroxidase activity. In this paper, porous hollow CuS nanospheres with a variety of sizes were fabricated by one-pot method based on a facile template-assisted hydrothermal approach. The size of the porous hollow CuS nanospheres could be simply tuned by adjusting the molar ratios of reactants, the reaction temperature and time. The as-prepared porous hollow CuS nanospheres were demonstrated to exhibit more prominent intrinsic peroxidase-like activity using TMB as a peroxidase substrate in presence of hydrogen peroxide (H_2O_2), as a significant comparison to previous reports, demonstrating that the new developed synthetic porous hollow CuS nanospheres can be a new kind of candidate for peroxidase mimics, and is promising for application in biosensors, environmental monitoring and so on.

1. Introduction

It has known that, natural enzymes, including horseradish peroxidase (HRP), share a basic defective feature that is also sensitive to environmental conditions like strong acidic, basic medium and high temperature and is difficult to be prepared in large quantities.[1] Therefore, interests in developing nano-scaled inorganic materials with peroxidase-like activity in the biochemical fields are rising, and it has been successful cases such as artificial mimic enzyme, including magnetic NPs,[2-4] carbon nanomaterials,[5-7] noble metal NPs,[8-10] some other composites and so on.[11, 12]

Metal chalcogenide clusters are interesting due to their unique optical, photovoltaic and catalytical properties etc.[13-16] Especially, the bio-applications of CuS nanomaterials are interesting and still remain big space for further sightseeing because of their high catalytic activity. For example, He et al. firstly reported that the Copper sulfide concave polyhedral superstructures (CuS CPSs) have an intrinsic enzyme mimetic activity similar to that of natural peroxidases such as HRP, as they can quickly catalyze the oxidation of HRP substrates 3,3',5,5'-tetramethylbenzidine (TMB) in the presence of H_2O_2.[17] Further reports include CuS nanoparticles as a mimic peroxidase for detecting glucose of human blood,[18] CuS-graphene composites for the colorimetric detection of H_2O_2,[19] Au/CuS composites catalyst with peroxidase-like activity for degrading a pollutant (Rhodamine 6G).[20] These reports are successful but can be further modified with the large-scale preparation of the CuS nanomaterials and high catalytic ability.

Porous hollow nanostructures have received considerable attention due to their unique properties, including the low material density, large surface area, void space compared to the nonporous hollow counterparts. As a result, porous hollow nanostructures have become one of the most promising candidates in catalysis, drug-delivery carriers and so on.[21-28]

Copper sulfide, an important semiconductor chalcogenide with unique optical and electronic properties, is a perspective material with wide applications in the fields of sensing,[29, 30] imaging and photothermal therapy,[31, 32] nanometer-scale switching,[33] solar cells and lithium-ion batteries and so on.[16, 34-39] To date, CuS nanoparticles have been synthesized with a wide repertoire of nanostructures such as 0D nanoparticles,[40] 1D nanotubes,[41, 42] nanowires,[43-45] and nanoneedles,[46] 2D nanoplates,[47, 48] and nanorods,[49] 3D porous hollow nanospheres,[50-52] nanocages,[25, 31] and nanoflowers.[53-55] Especially, the properties of synthetic CuS material can be tuned by tailoring the structure and morphology. Till now, reported methods of synthesis of CuS materials have included hydrothermal and solvothermal preparations,[17, 56] electron and microwave irradiation,[57, 58] sonochemical synthesis,[59, 60] template-assisted methods and so on.[61-64]

In case of porous hollow CuS nanostructures, template-assisted method has been favoured highly by researchers. In particularly, the sacrificial template-directed chemical transformation method based on the Kirkendall effect has been demonstrated to be an effective approach for the synthesis of porous hollow CuS nanostructures.[22, 65, 66] It is worth noting that the sacrificial template-directed chemical transformation method has the advantages without modification of the template surface.[63] The reactive sacrificial templates, which act as both reactive precursors and templates, have to be removed by Kirkendall diffusion in the core. The morphologic control of objective reaction products and the occurrence of chemical reaction on their surface have to be simultaneously processed.[62] That is, how to prepare the templates of the sacrificial template-

directed strategy is critical for expected porous hollow nanostructures with designed morphologies and controllable pore size. Although, various inorganic porous hollow structures have been successfully prepared by employing reactive sacrificial templates,[67-70] multiple steps are usually required, which are time-consuming and complex. In other words, it remains a challenge to achieve size-controlled synthesis of porous hollow CuS nanospheres by employing a general sacrificial template.

In such case, a facile one-pot and template-assisted hydrothermal method was developed to synthesize porous hollow CuS nanomaterials with low cost and prominent peroxidase-like activity (Scheme 1). Study found that the size of porous hollow CuS nanospheres could be tuned by multi-channel such as reaction temperature, time and precursor ratio. What's more, we verified that synthetic porous hollow CuS nanomaterials showed extremely prominent intrinsic peroxidase activity, and it can quickly catalyze TMB oxidation in the presence of H_2O_2. Furthermore, our synthetic porous hollow CuS nanomaterials, acting as a mimic peroxidase, exhibited excellent catalytic properties, stability, and dispersibility compared to HRP.

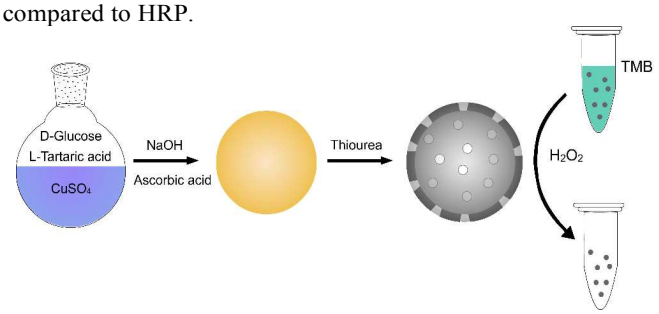

Scheme 1. Schematic illustration of the formation of porous hollow CuS nanospheres and the oxidation color reaction of TMB.

2. Experimental section

2.1 Materials

Copper nitrate pentahydrate($Cu(NO_3)_2$•$5H_2O$), D-Glucose, 30wt% hydrogen peroxide (H_2O_2), DL-Tartaric acid were all purchased from Chengdu Kelong Chemical Co., Ltd., (Chengdu, China). Sodium hydroxide (NaOH), ethanol (C_2H_5OH), thiourea were obtained from Chongqing Chuandong Chemical Co., Ltd., (Chongqing, China). Ascorbic acid was purchased from Beijing Dingguo Changsheng Biotechnology Co., Ltd., (Beijing, China). Polyvinylpyrrolidone (PVP, *Mw*=55000) was received in standard grade from Sigma-Aldrich Chemical Co., Ltd., (America). 3,3′,5,5′-tetramethylbenzidine dihydrochloride (TMB) was obtained from Aladdin Industrial Co., Ltd., (Shanghai, China). Double distilled water was used throughout the experiment.

2.2 Synthesis of porous hollow CuS nanospheres

Porous hollow CuS nanospheres were synthesized by a facile one-pot method with carefully controlling reaction time. In a typical procedure, 25 μmol $Cu(NO_3)_2$, 100 μmol DL-Tartaric acid and 0.1 g PVP were dissolved in 20 mL deionized water and stirred 1100 r/min at 65 °C in a water bath. After 5 min, 275 μmol NaOH was added to the aqueous solution, the color of the solution became dark blue instantly. After 5 min, 25 μmol D-Glucose and 50 μmol Ascorbic acid were quickly added to the dark blue aqueous solution, resulting to orange precipitates quickly. After 5 min, 25 μmol thiourea was quickly added to the system, and then the flask was placed quickly into an oil bath, and stirred 1000 r/min at 85 °C for 6 h. Finally, the resulting black precipitates were centrifuged and washed sequentially with ethyl alcohol and deionized water, and dried under vacuum at 50 °C for 8 h.

2.3 The detection of OH•

To verify that OH• was generated in this process, 5,5-dimethyl-1-pyrroline-N-oxide (DMPO) was used as a specific target molecule, which was widely used in the detection of OH•. After adding a suitable amount of porous hollow CuS nanospheres, DMPO could react with OH• to yield DMPO-OH, which was measured by the electron spin resonance spectrophotometry (ESRS).

2.4 Peroxidase-like activity evaluation

To assess the peroxidase-like activity of porous hollow CuS nanospheres, the catalytic oxidation of the peroxidase substrate TMB was performed in the presence of H_2O_2 to produce a blue color reaction. In order to examine the capability of porous hollow CuS nanospheres as peroxidase catalyst for the oxidation of TMB, 50 μl of 30wt% H_2O_2 and 30 μl of 10 mM TMB were added to 3 ml deionized water. Then, once a certain amount of the CuS suspension was added to the above mixture, the oxidation progress was quickly initiated. All the reactions were monitored at 30 s intervals at 25 °C by recording the absorption spectra in time-scan mode at 653 nm.

2.5 Apparatus and characterization

The crystallographic structure of as-prepared products was analyzed by X-ray diffractometer (XRD, D8 Advance, Bruker, Germany), while their morphology were measured with an S-4800 scanning electron microscopy (FESEM, Hitachi, Japan) equipped with an energy-dispersive X-ray spectroscopy (EDS) system and a high resolution transmission electron microscopy (HRTEM, Tecnai G2 F20 S-TWIN, FEI Company, USA), respectively. Ultraviolet-visible (UV-vis) spectra were recorded on a UV-vis spectrophotometer (UV3600, Shimadzu, Japan). X-ray photoelectron spectrometer (XPS, Escalab 250Xi, Thermo, USA) was used to measure the composition of porous hollow CuS nanospheres. The Brunauer-Emmett-Teller specific surface area of the powders was performed by nitrogen adsorption apparatus (BET, AS1-MP-9, Quantachrome, USA). Electron paramagnetic resonance (EPR) spectra were measured on a Bruker spectrometer (ESP-300E, Bruker, Germany) at room temperature.

3. Results and Discussion

3.1 Strategy for the design of the porous hollow structure.

According to the Kirkendall effect, porous hollow CuS nanospheres synthesized by template-assisted method was illusrated in the schema. Firstly, it is very key that the size-controllable Cu_2O templates are synthesized under certain conditions, which completely determine the size of CuS hollow. Then an shell of CuS is formed on the outside surface of the Cu_2O templates with the adding of precursor. Secondly, under the driving force of the concentration gradient, the diffusion velocity of copper ions from inside to outside is faster than that of sulfur ions from outside to inside through the CuS shell. As a result, the Cu_2O core gradually

disappears, and the porous CuS shell gradually forms. With the increasing of the reaction time, the porous hollow CuS nanospheres with size-controllable porous hollow structure are synthesized, which is simply tuned by adjusting the molar ratios of reactants, the reaction temperature and time.

3.2 Physical characterizations.

The SEM (Fig. 1a-b) and TEM images (Fig. 1d-e) of the as-prepared porous hollow CuS nanospheres clearly exhibited that they have excellent dispersity and regular morphology, with a uniform diameter of approximate 200 nm. It was further found that some small nanoparticles can be seen on the surface of the porous hollow CuS nanospheres, hence the formation of rough surfaces of the shells can be successfully achieved, and a few of nanoparticles had solid Cu_2O core from Fig. 1d-e, which can be due to the inadequate reaction. The magnified TEM image of the as-prepared samples is proved (Fig. 1f) that their rough shells composed of nanoparticles, with a void inside. Especially, an extremely strong contrast difference between the dark edge and the pale center indicates the as-prepared CuS nanospheres with porous hollow interior. Furthermore, the shell thickness of porous hollow CuS nanospheres is approximate 30 nm from Figure 1f. The clearly lattice fringes (Fig. 1c) displayed that the porous hollow CuS nanospheres have well-defined crystal structure. The corresponding lattice spacing is 0.312 nm, which is in good agreement with standard d value of the interlayer spacing of the (102) crystallographic plane of hexagonal CuS.

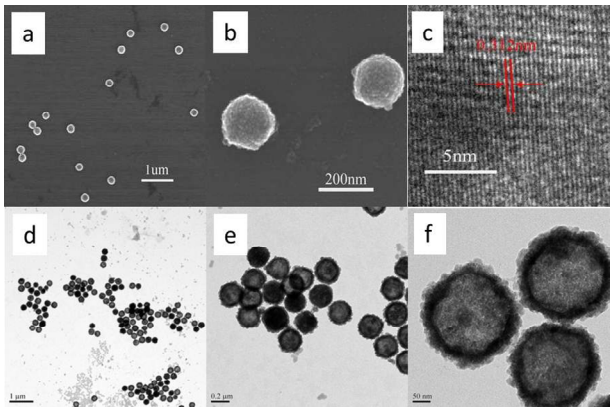

Fig. 1 Morphology and structure characterization of porous hollow CuS nanospheres. (a) SEM, (b) magnified SEM (c) HRTEM, (d-f) different magnification TEM image of porous hollow CuS nanospheres.

The purity, phase, crystallinity, and composition of as-prepared products are initially determined by XRD and XPS (Fig. 2). The XRD pattern of the porous hollow CuS nanospheres shown in Figure 2a indicated that all the primary diffraction peaks of the as-synthesized CuS mesospheres under hydrothermal experimental conditions are consistent with the standard data of hexagonal CuS (JCPDS no.00-006-0464). They have the P63/mmc space group and a primitive hexagonal unit cell with a = b = 3.792 Å and c = 16.34 Å, and possess a pure phase. No other obvious peaks of impurities are observed in the sample, and the several stronger diffraction peaks located at 29.28, 31.79, 32.82, 47.95 and 59.34 were respectively attributed to (102), (103), (006), (110) and (116) planes. That is, the porous hollow CuS nanospheres prepared by a template-assisted and one-pot method had a good crystallinity.

Figure 2b-c exhibits the high-resolution XPS spectra of Cu and S in the 2p region, respectively. Figure 2b shows the binding energies of Cu $2p_{3/2}$ and Cu $2p_{1/2}$ slightly left-shift to 932.23 and 952.18 eV and two weak satellite peaks at 943.2 and 963.6 eV are disappeared, respectively, indicating the presence of the typical Cu^{2+} and little Cu^{+} in the samples.[21] The change in binding energy of Cu 2p are caused by the charging of copper element valence. That is, a small amount of Cu^{2+} in CuS is reduced to Cu_2S. Meanwhile, as shown in Figure 2c, the binding energies of S $2p_{3/2}$ and S $2p_{1/2}$ peaks are at 161.98 and 162.88 eV, respectively, indicating the presence of S^{2-} in the prepared samples.[71] In a word, the purity of the as-prepared porous hollow CuS nanospheres is high.

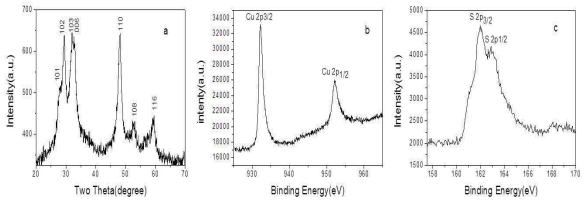

Fig. 2 Composition and structure characterizations of porous hollow CuS nanospheres. (a) XRD, (b) and (c) XPS spectrum of porous hollow CuS nanospheres.

To verify the as-synthesized CuS nanospheres with larger specific surface area, The BET surface area and pore volume are 33 m^2 g^{-1} and 0.19 cm^3 g^{-1}, respectively. Figure 3a shows nitrogen adsorption-desorption isotherms of the CuS nanospheres exhibit representative type IV curves, which indicates the presence of mesopores and macropores in the CuS nanospherical shell and core. Figure 3b shows that the front end of the curve is the pore size distribution of CuS nanospherical shell, and the back end of the curve is the pore size distribution of CuS nanospherical hollow, which are consistent with the nitrogen adsorption-desorption isotherms of the CuS nanospheres. These verified that the porous hollow CuS nanospheres possessed very good hollow structure, in accordance with the TEM results. In view of the above analysis, the porous hollow structure of the as-prepared samples has larger specific surface area than CuS caved superstructures[72], which, as solid catalyst, can provide more active sites in liquid-solid catalytic reaction process. and further confirms the larger specific surface area of the porous hollow CuS nanospheres.

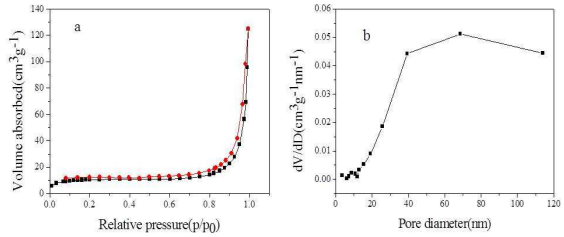

Fig. 3 Nitrogen adsorption−desorption isotherms (a) and pore size distribution (b) of the obtained porous hollow CuS nanospheres.

3.3 The size control of the porous hollow CuS nanomaterials.

Following above synthetic procedures, monodisperse porous hollow CuS nanospheres with different size could be synthesized by adjusting the reaction conditions. Figure 4 shows the SEM and TEM images of CuS products synthesized at reaction temperature of 50 °C, 65 °C and 80 °C for 10 min in a water bath, respectively, indicating that these porous hollow CuS nanomaterials are quite uniform, monodispersed and hollow spherical, and their rough surfaces composed of many

regular nanoparticles. With increasing of the reaction temperature from 50 °C to 80 °C, the average diameter of the porous hollow nanospheres is found to be reduced from approximate 420 nm (50 °C) to approximate 250 nm and 180 nm at 65 °C and 80 °C. It implies that a higher reaction temperature is suitable to grow smaller diameter of the porous hollow CuS nanospheres. Liu et al. also obtained different diameter $Cu_{2-x}S$ nanoparticle at different reaction temperature. For example, 2.8 nm $Cu_{2-x}S$ nanoparticles were synthesized at 140 °C and temperature was held at 132 °C for about 2 min. 6.8 nm $Cu_{2-x}S$ nanoparticles were also prepared at 115 °C, and the temperature was held at 100 °C for about 3 min. The monodisperse growth of CuS nanospheres ascribes the size-focusing effect expressed by the equation, where V' is the rate of volume growth of a nanocrystal, d is the diameter and d' is the linear growth rate. In the initial stages of reaction, following a burst of nucleation, particle growth is limited by diffusion of monomers to nuclei, and the higher reaction temperature, the faster diffusion speed, resulting in a constant V'. With the extension of reaction time, nuclei quickly assemble into nanoparticle. Under these conditions, smaller nanoparticles have higher d' than larger nanoparticles and therefore tend to catch up with larger particles.[73] Monodispersed porous hollow CuS nanospheres with tunable size crystal nanostructure can be achieved by adjusting the reaction temperature. That is, reaction temperature is an important factor in determining the size of CuS nanospheres.

$$v' = \frac{\pi}{2}(d^2)d' = constant \qquad (1)$$

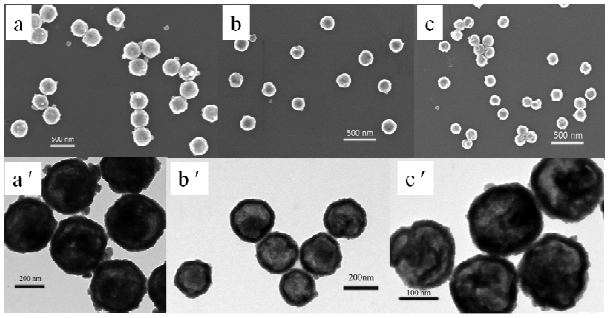

Fig. 4 SEM (a), (b), (c) and TEM (a′), (b′), (c′) images of synthesized porous hollow CuS nanospheres at the reaction temperature of 50 °C, 65 °C and 80 °C for 10min.

We further investigated the effect of reaction time on the size of the porous hollow CuS nanospheres. Figure 5 shows the SEM and TEM images of the porous hollow CuS nanospheres obtained after reaction of 5, 10 and 15 min, respectively, and indicates synthesized nanomaterials have regular diameter change and hollow structure. The diameter of the CuS nanospheres is measured to be approximate 200, 250 and 350 nm, respectively. Two important observations are made on the growth of the CuS nanospheres with increasing the reaction time. Firstly, the diameter the CuS nanospheres is increased with the extension of reaction time. Secondly, small nanoparticles gradually disappear, and the formation of pits on the surface of CuS nanospheres is found in figure 5c, which apparently needs more detailed work for the reason of pits formation. Sun et al. reported that ethanol molecules can lead to the formation of pits on (111) facets of Cu_2O.[74] In a word, reaction time also plays a key role in deciding the diameter of the porous hollow CuS nanospheres.

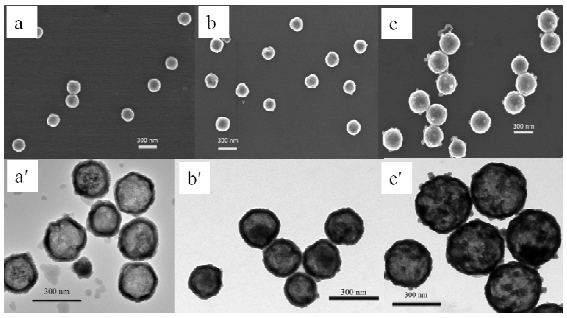

Fig. 5 SEM (a), (b), (c) and TEM (a′), (b′), (c′) images of synthesized porous hollow CuS nanospheres for reaction time of 5 min, 10 min and 15 min.

In such case, we can further estimate the effect of precursor ratios on the size and morphology of products, and thus three different molar ratios of $Cu(NO_3)_2$ and Vc (1:1, 1:2 and 1:3) were used. Figure 6 shows the size and morphology of CuS nanomaterials obtained with $Cu(NO_3)_2$ and Vc molar ratios of 1:1, 1:2 and 1:3, respectively. With a 1:1 molar ratio, the monodisperse polyhedral CuS nanoparticles were obtained in Figure 6a. It is assumed that atoms located on the edges and corners are unsaturated and should have higher surface energy, so they are more easily etched,[75] which could results in the formation of the polyhedral CuS nanoparticles with the size of around 300 nm. With a 1:2 molar ratio, the monodisperse CuS nanospheres were obtained. The reason can be the edges and corners of the polyhedral CuS nanoparticles are further etched, resulting in the formation of the approximate 200 nm nanospheres (Fig. 6b). When the molar ratio of $Cu(NO_3)_2$ and Vc is increased to 1:3, the uniform CuS nanospheres with pits are formed, and the diameter of these nanospheres are measured to be around 180 nm, as shown in Figure 6c. Therefore, it can be concluded that the precursor ratios can have a significant role in the size and morphology change of CuS nanostructures.

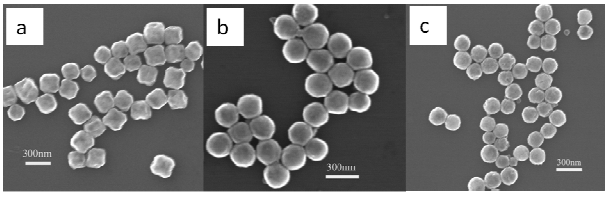

Fig. 6 SEM images of synthesized porous hollow CuS nanospheres for precursor (a) $Cu(NO_3)_2$:Vc = 1:1, (b) $Cu(NO_3)_2$:Vc = 1:2 and (c) $Cu(NO_3)_2$:Vc =1:3.

3.4 Peroxidase-like catalytic activity of porous hollow CuS nanospheres.

As far as we know, there are no previous reports on the prominent peroxidase-like activity research of the porous hollow CuS nanospheres. Considering their special structures, the peroxidase-like activity of the as-prepared porous hollow CuS nanospheres was firstly investigated through the catalytic oxidation of the TMB in the presence of H_2O_2. TMB can be oxidized to produce a typical blue color substance in the presence of H_2O_2 (Fig.7a inset). As shown in Figure 7a, the catalytic reaction can be monitored by following the changing of absorbance (*Abs*) at 653 nm at room temperature, which is originated from the oxidation product of TMB. The absorbance increased quickly with increasing the reaction time, which indicated that the porous hollow CuS nanospheres indeed exhibited high peroxidase-like catalytic activity toward TMB oxidation. Fig. 7b shows the change of TMB *Abs* at different conditions by plotting

Abs as a function of time. Curve a represented the control experiment without any catalyst, which showed that the *Abs* was very low at 653 nm in TMB-H_2O_2 system. With increasing of the porous hollow CuS nanospheres dose, we found the *Abs* value of solution increased obviously in TMB-CuS-H_2O_2 system (curve c, d and e) in 7 min. In comparison with curve a, the *Abs* at 653 nm increased dramatically with the addition of different dose CuS, which indicated that the peroxidase-like catalytic activity of the porous hollow CuS nanospheres is highly dependent on the concentration. Furthermore, the possible reason of the porous hollow CuS nanospheres with the very outstanding peroxidase-like activity was resulting from their larger specific surface area.

To verify the observed peroxidase-like activity was attributed to the intact nanoparticles, it is important to rule out the possibility that the observed catalytic activity is caused by copper ions leaching from the porous hollow CuS nanospheres in the solution. Leaching solution was obtained by incubating the porous hollow CuS nanospheres solution for 0.5 h under ultrasonication, and then the porous hollow CuS nanospheres were removed from solution by centrifugation. As shown in Figure 7b, curve b represented the leaching solution experiment, which showed similar *Abs* to the control experiment. That is, leaching solution experiment verified that few copper ions were leached in the leaching solution, and the observed peroxidase-like activity is due to the intact porous hollow CuS nanospheres.

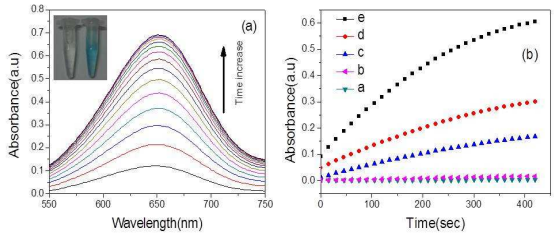

Fig. 7 UV-vis absorption curves of TMB solutions oxidized recorded on 7 min of the catalytic reaction. (a) UV-vis absorption curves of TMB–H_2O_2 system catalyzed by porous hollow CuS nanospheres. (The inset is the typical photograph of TMB before and after oxidation) (b) Time dependent absorbance curves at 653 nm after the addition of different doses of porous hollow CuS nanospheres (Curves a, b, c, d and e represent the control experiment without any catalyst, the leaching solution experiment and 1.2, 3, 6 μg ml^{-1} CuS catalytic experiment, respectively.)

We also investigated the effect of the size on the catalytic activity of the porous hollow CuS nanospheres and the results are shown in Figure 8A. In comparison, curve a and c showed that 180 nm CuS nanospheres exhibited about three times higher activity than 420 nm CuS nanospheres, and curve a and b showed 250 nm CuS nanospheres also showed slightly lower catalytic activity than 180 nm CuS nanospheres. The reason may be that the small porous hollow CuS nanospheres have higher surface area than the big. The finding verified that the catalytic activity of the porous hollow CuS nanospheres could been adjusted effectively by varying the particle size. We also investigated the reusability of our porous hollow CuS catalyst. The XRD pattern showed that the crystallinity and phase of the porous hollow CuS nanomaterials remained basically unchanged after five reaction cycles, but the corresponding peak intensities decreased in comparison to that of CuS nanomaterials before the reaction(Fig. 8B). The reason may be that the part of CuS nanomaterials were corroded by H_2O_2 in the process of catalytic reaction. In a word, Fig.8B indicates that our porous hollow CuS nanomaterials are basically stable, making this type of material a potential candidate for a recyclable peroxidase-like activity reagent.

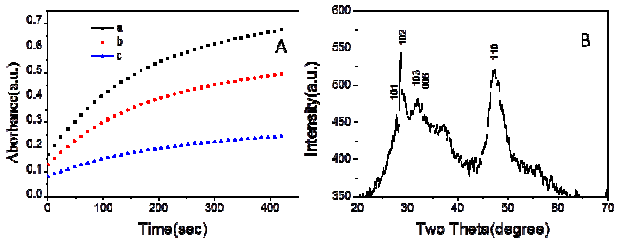

Fig. 8 (A) Time dependent absorbance curves at 653 nm after the addition of different size porous hollow CuS nanospheres at the same concentration: (a) 180 nm, (b) 250 nm (c) 420 nm. (the concentration of different size porous hollow CuS nanospheres is 6 mg ml-1), (B) The XRD pattern of the porous hollow CuS nanospheres after catalytic reaction for five cycles.

The excellent intrinsic peroxidase-like activity of the porous hollow CuS nanospheres making the oxidation of TMB quickly (Fig. 7) might be ascribed to the yield of hydroxide radicals and follows following reaction mechanism.[18, 20]

$$Cu^{2+} + H_2O_2 \rightarrow H^+ + CuOOH^+ \quad (2)$$

$$CuOOH^+ \rightarrow HOO\bullet + Cu^+ \quad (3)$$

$$Cu^+ + H_2O_2 \rightarrow Cu^{2+} + OH\bullet + OH^- \quad (4)$$

In order to verify that OH• was generated from the decomposition of H_2O_2 in the presence of CuS peroxidase catalysis, the electron spin resonance (ESR) technique was used to detect oxygen-related radicals because of their short lifetime. 5,5-dimethyl-1-pyrroline-N-oxide (DMPO) was used as a specific target molecule to capture OH• in the detection process of OH•. The obvious signal intensity enhancement of the ESR spectra in the presence of the porous hollow CuS nanospheres strongly suggested that a high amount of OH• was generated in the peroxidase catalytic reaction (Fig. 9). In other words, the as-synthesized porous hollow CuS nanospheres have excellent intrinsic peroxidase-like activity to accelerate the decomposition of H_2O_2 to generate a high yield of OH• on their surface.

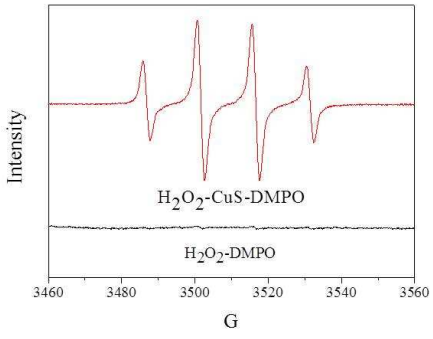

Fig. 9 DMPO−OH• adduct in the presence (red line) or absence (blackline) of porous hollow CuS nanospheres. Conditions: modulation amplitude, 1.944 G; microwave power, 1.002e + 001 mW; receiver gain, 1.00e + 005; sweep width, 100.00 G. The ESR measurements were achieved with a Bruker ESP-300E spectrometer operating in the X-band at room temperature.

Conclusions

In summary, the porous hollow CuS nanomaterials with well-defined

morphology have been successfully synthesized via a simple one-pot method by employing a general sacrificial template process with low-cost. The as-prepared CuS nanomaterials with unique porous hollow structure were verified to possess outstanding peroxidase-like activity to catalyze the oxidation of typical peroxidase substrates (TMB) in the presence of H_2O_2. According to practical requirements for the diameter of CuS nanomaterials, the diameter of porous hollow CuS nanospheres could be tuned easily by multi-channel such as reaction temperature, time and precursor ratio. Moreover, the study also demonstrated the observed peroxidase-like activity was attributed to the intact nanoparticles, not by copper ions leaching similar to Fe_3O_4 and FeS. The research of peroxidase-like activity on CuS further indicated that the as-prepared porous hollow CuS nanospheres as an artificial enzyme could have potential applications in biosensors, immunoassays, biocatalysis and environmental monitoring.

Acknowledgements

This work was partially supported by the National Natural Science Foundation of China (NSFC, No. 21375109) and the Cultivation Plan of Chongqing Science & Technology Commission for 100 Outstanding Science and Technology Leading Talents. Also, this work was financially supported by the Fundamental Research Funds for the Central Universities of China (No. XDJK2013C036)

Notes and references

[a]*Key Laboratory of Luminescent and Real-Time Analytical Chemistry, Ministry of Education, College of Chemistry and Chemical Engineering, Southwest University, Chongqing 400715. E-mail: chengzhi@swu.edu.cn; Fax/Tel: (+86)-23-68254659.*

[b]*College of Pharmaceutical Sciences, Southwest University, Chongqing 400715, PR China*

[c]*College of Chemical Engineering, Guizhou University of Engineering Science, Guizhou 551700, PR China.*

1. G. Wulff, *Chem. Rev.*, 2001, **102**, 1-28.
2. G. Guan, L. Yang, Q. Mei, K. Zhang, Z. Zhang and M.-Y. Han, *Anal. Chem.*, 2012, **84**, 9492-9497.
3. J. Yin, H. Cao and Y. Lu, *J. Mater. Chem.*, 2012, **22**, 527-534.
4. J. Qian, X. Yang, L. Jiang, C. Zhu, H. Mao and K. Wang, *Sensor. Actuat. B-Chem.*, 2014, **201**, 160-166.
5. Y. Song, K. Qu, C. Zhao, J. Ren and X. Qu, *Adv. Mater.*, 2010, **22**, 2206-2210.
6. W. Shi, Q. Wang, Y. Long, Z. Cheng, S. Chen, H. Zheng and Y. Huang, *Chem. Commun.*, 2011, **47**, 6695-6697.
7. R. Cui, Z. Han and J.-J. Zhu, *Chem–Eur. J.*, 2011, **17**, 9377-9384.
8. Y. Zhang, C. Xu, B. Li and Y. Li, *Biosens. Bioelectron.*, 2013, **43**, 205-210.
9. Y.-T. Zhou, W. He, W. G. Wamer, X. Hu, X. Wu, Y. M. Lo and J.-J. Yin, *Nanoscale*, 2013, **5**, 1583-1591.
10. X. Chen, B. Su, Z. Cai, X. Chen and M. Oyama, *Sensor. Actuat. B-Chem.*, 2014, **201**, 286-292.
11. A. K. Dutta, S. K. Maji, D. N. Srivastava, A. Mondal, P. Biswas, P. Paul and B. Adhikary, *ACS Appl. Mater. Inter.*, 2012, **4**, 1919-1927.
12. J. Zhao, Y. Xie, W. Yuan, D. Li, S. Liu, B. Zheng and W. Hou, *J. Mater. Chem. B*, 2013, **1**, 1263-1269.
13. W. L. Li, S. Q. Lie, Y. Q. Du, X. Y. Wan, T. T. Wang, J. Wang and C. Z. Huang, *J. Mater. Chem. B*, 2014, **2**, 7027-7033.
14. S. Q. Lie, D. M. Wang, M. X. Gao and C. Z. Huang, *Nanoscale*, 2014, **6**, 10289-10296.
15. S. Q. Lie, H. Y. Zou, Y. Chang and C. Z. Huang, *RSC Adv.*, 2014, **4**, 55094-55099.
16. Z. Liu, J. Han, L. Han, K. Guo, Y. Li, T. Cui, B. Wang and X. Liang, *Mater. Chem. Phys.*, 2013, **141**, 804-809.
17. W. He, H. Jia, X. Li, Y. Lei, J. Li, H. Zhao, L. Mi, L. Zhang and Z. Zheng, *Nanoscale*, 2012, **4**, 3501-3506.
18. A. K. Dutta, S. Das, S. Samanta, P. K. Samanta, B. Adhikary and P. Biswas, *Talanta*, 2013, **107**, 361-367.
19. G. Nie, L. Zhang, X. Lu, X. Bian, W. Sun and C. Wang, *Dalton T.*, 2013, **42**, 14006-14013.
20. Q. Cai, S. Lu, F. Liao, Y. Li, S. Ma and M. Shao, *Nanoscale*, 2014, **6**, 8117-8123.
21. J. Zhang, J. Yu, Y. Zhang, Q. Li and J. R. Gong, *Nano Lett.*, 2011, **11**, 4774-4779.
22. S. Sun, X. Song, C. Kong, D. Deng and Z. Yang, *CrystEngComm*, 2012, **14**, 67-70.
23. J. Kundu and D. Pradhan, *ACS Appl. Mater. Inter.*, 2014, **6**, 1823-1834.
24. E. Hong, D. Kim and J. H. Kim, *J. Ind. Eng. Chem.*, 2014, **20**, 3869-3874.
25. S. Ramadan, L. Guo, Y. Li, B. Yan and W. Lu, *Small*, 2012, **8**, 3143-3150.
26. Y.-Q. Zhang, B.-P. Zhang and L.-F. Zhu, *RSC Adv.*, 2014, **4**, 59185-59193.
27. M. Tanveer, C. Cao, I. Aslam, Z. Ali, F. Idrees, M. Tahir, W. S. Khan, F. K. Butt and A. Mahmood, *RSC Adv.*, 2014, **4**, 63447-63456.
28. X. Meng, G. Tian, Y. Chen, R. Zhai, J. Zhou, Y. Shi, X. Cao, W. Zhou and H. Fu, *CrystEngComm*, 2013, **15**, 5144-5149.
29. J. Bai and X. Jiang, *Anal. Chem.*, 2013, **85**, 8095-8101.
30. X. Zhang, G. Wang, A. Gu, Y. Wei and B. Fang, *Chem. Commun.*, 2008, 5945-5947.
31. Y. Wang, Y. Xiao, H. Zhou, W. Chen and R. Tang, *RSC Adv.*, 2013, **3**, 23133-23138.
32. Z. Zha, S. Zhang, Z. Deng, Y. Li, C. Li and Z. Dai, *Chem. Commun.*, 2013, **49**, 3455-3457.
33. T. Sakamoto, H. Sunamura, H. Kawaura, T. Hasegawa, T. Nakayama and M. Aono, *Appl. Phys. Lett.*, 2003, **82**, 3032-3034.
34. L. Monconduit, *J. Phys. Chem. C*, 2014, **118**, 10531-10544.
35. M. Nagarathinam, K. Saravanan, W. L. Leong, P. Balaya and J. J. Vittal, *Cryst. Growth Des.*, 2009, **9**, 4461-4470.
36. F. Wu, J. Chen, R. Chen, S. Wu, L. Li, S. Chen and T. Zhao, *J. Phys. Chem. C*, 2011, **115**, 6057-6063.
37. L. Quan, W. Li, L. Zhu, X. Chang and H. Liu, *RSC Adv.*, 2014, **4**, 32214-32220.
38. R. K. Bhosale, S. A. Agarkar, I. Agrawal, R. A. Naphade and S. Ogale, *RSC Adv.*, 2014, **4**, 21989-21996.
39. S.-i. Eda, K. Moriyasu, M. Fujishima, S. Nomura and H. Tada, *RSC Adv.*, 2013, **3**, 10414-10419.
40. X. Dong, D. Potter and C. Erkey, *Ind. Eng. Chem. Res.*, 2002, **41**, 4489-4493.
41. Q. Lu, F. Gao and D. Zhao, *Nano Lett.*, 2002, **2**, 725-728.
42. L. Qian, X. Tian, L. Yang, J. Mao, H. Yuan and D. Xiao, *RSC Adv.*, 2013, **3**, 1703-1708.
43. A. Ghahremaninezhad, E. Asselin and D. G. Dixon, *J. Phys. Chem. C*, 2011, **115**, 9320-9334.
44. X. Qian, H. Liu, N. Chen, H. Zhou, L. Sun, Y. Li and Y. Li, *Inorg. Chem.*, 2012, **51**, 6771-6775.
45. P. Xue, R. Lu, D. Li, M. Jin, C. Tan, C. Bao, Z. Wang and Y. Zhao, *Langmuir*, 2004, **20**, 11234-11239.
46. T. Zhu, B. Xia, L. Zhou and X. Wen Lou, *J. Mater. Chem.*, 2012, **22**, 7851-7855.
47. L. Chu, B. Zhou, H. Mu, Y. Sun and P. Xu, *J. Cryst. Growth*, 2008, **310**, 5437-5440.
48. L. Liu, H. Zhong, Z. Bai, T. Zhang, W. Fu, L. Shi, H. Xie, L. Deng and B. Zou, *Chem. Mater.*, 2013, **25**, 4828-4834.
49. P. Roy, K. Mondal and S. K. Srivastava, *Cryst. Growth Des.*, 2008, **8**, 1530-1534.
50. K. Dong, Z. Liu, Z. Li, J. Ren and X. Qu, *Adv. Mater.*, 2013, **25**, 4452-4458.
51. X. L. Yu, C. B. Cao, H. S. Zhu, Q. S. Li, C. L. Liu and Q. H. Gong, *Adv. Funct. Mater.*, 2007, **17**, 1397-1401.
52. S. Xiong and H. C. Zeng, *Angewandte Chemie*, 2012, **124**, 973-976.
53. T.-Y. Ding, M.-S. Wang, S.-P. Guo, G.-C. Guo and J.-S. Huang, *Mater. Lett.*, 2008, **62**, 4529-4531.
54. X.-H. Guan, P. Qu, X. Guan and G.-S. Wang, *RSC Adv.*, 2014, **4**, 15579-15585.
55. W. P. Lim, H. Y. Low and W. S. Chin, *Cryst. Growth Des.*, 2007, **7**, 2429-2435.
56. Z. Cheng, S. Wang, Q. Wang and B. Geng, *CrystEngComm*, 2010, **12**,

144-149.
57. J. Liu and D. Xue, *J. Mater. Chem.*, 2011, **21**, 223-228.
58. X. Yan, E. Michael, S. Komarneni, J. R. Brownson and Z.-F. Yan, *Ceram. Int.*, 2013, **39**, 4757-4763.
59. J. Shi, X. Zhou, Y. Liu, Q. Su, J. Zhang and G. Du, *Mater. Lett.*, 2014, **126**, 220-223.
60. H. Xu, W. Wang and W. Zhu, *Mater. Lett.*, 2006, **60**, 2203-2206.
61. Z.-h. Yang, D.-p. Zhang, W.-x. Zhang and M. Chen, *J. Phys. Chem. Solids*, 2009, **70**, 840-846.
62. J. Gao, Q. Li, H. Zhao, L. Li, C. Liu, Q. Gong and L. Qi, *Chem. Mater.*, 2008, **20**, 6263-6269.
63. H. Zhu, J. Wang and D. Wu, *Inorg. Chem.*, 2009, **48**, 7099-7104.
64. S. Wan, F. Guo, L. Shi, Y. Peng, X. Liu, Y. Zhang and Y. Qian, *J. Mater. Chem.*, 2004, **14**, 2489-2491.
65. C. Deng, X. Ge, H. Hu, L. Yao, C. Han and D. Zhao, *CrystEngComm*, 2014, **16**, 2738-2745.
66. S. Sun, X. Song, C. Kong, S. Liang, B. Ding and Z. Yang, *CrystEngComm*, 2011, **13**, 6200-6205.
67. J. Yang, L. Qi, C. Lu, J. Ma and H. Cheng, *Angew. Chem. Int. Edit.*, 2005, **44**, 598-603.
68. H. Cao, X. Qian, C. Wang, X. Ma, J. Yin and Z. Zhu, *J. Am. Chem. Soc.*, 2005, **127**, 16024-16025.
69. S. Jiao, L. Xu, K. Jiang and D. Xu, *Adv. Mater.*, 2006, **18**, 1174-1177.
70. S. Peng and S. Sun, *Angew. Chem. Int. Edit.*, 2007, **46**, 4155-4158.
71. T. Kuzuya, K. Itoh, M. Ichidate, T. Wakamatsu, Y. Fukunaka and K. Sumiyama, *Electrochim. Acta*, 2007, **53**, 213-217.
72. Q. W. Shu, J. Lan, M. X. Gao, J. Wang and C. Z. Huang, *CrystEngComm*, 2014. **DOI:** 10.1039/C4CE02120G.
73. X. Liu, X. Wang, B. Zhou, W.-C. Law, A. N. Cartwright and M. T. Swihart, *Adv. Funct. Mater.*, 2013, **23**, 1256-1264.
74. S. Sun, H. You, C. Kong, X. Song, B. Ding and Z. Yang, *CrystEngComm*, 2011, **13**, 2837-2840.
75. L. Zhang, J. Shi, M. Liu, D. Jing and L. Guo, *Chem. Commun.*, 2014, **50**, 192-194.